# Triplet-State Electron Spin Resonance of Chlorophyll a and b Molecules and Complexes in PMMA and MTHF

## I: Experimental Determination of Fine-Structure and Rate Constants

W. Hägele, D. Schmid and, H. C. Wolf

Physikalisches Institut, Teil 3, Universität Stuttgart, 7000 Stuttgart, Germany

Z. Naturforsch. **33a**, 83–93 (1978); received November 4, 1977

The triplet state zero-field splittings and the rate constants for the population and depopulation of the triplet spin sublevels have been investigated for chlorophyll a and chlorophyll b in polymethylmethacrylate (PMMA) and methyltetrahydrofurane (MTHF) as a function of the concentration. In PMMA both chlorophyll a and chlorophyll b yielded only one ESR spectrum in the entire range of concentration which could be covered ($1.5 \times 10^{-5} - 1 \times 10^{-3}$ mole/l). In MTHF the results were more complicated. At low concentrations (up to $10^3$ mole/l) only one spectrum was observed, at higher concentrations additional spectra were detectable (all together two for chlorophyll a and five for chlorophyll b at $10^{-1}$ mole/l). The assignment of these spectra was facilitated by observing the "triplet resonance-field identity" which connects the resonance-field strengths for the canonical orientations of one particular species. Furthermore, the rate constants for some of these species could be determined.

### 1. Introduction

Electron spin resonance (ESR) experiments have proved to be a powerful tool for the investigation of the electronic and structural properties of molecules in their metastable triplet state. In recent years this technique has been applied increasingly to molecules which play a major role in the primary steps of photosynthesis, like chlorophyll, both in vivo [1–14] and in vitro [15–22]. These pigment molecules participate in at least three steps of the photosynthetic process: the so-called light harvesting, the transfer of the absorbed energy to the reaction center, and the actual charge separation. It has been suggested that the different roles of the chlorophyll molecules in the photosynthetic process are induced by different environments or by formation of complexes containing the pigment molecules [23–25].

In order to contribute to the solution of this question we have studied the ESR of chlorophyll a (chl a) and chlorophyll b (chl b) at various concentrations in a polar and a nonpolar solvent (MTHF and PMMA, respectively). It is the purpose of this work to investigate the influence of the environment and the concentration on the molecular properties of chlorophyll a and chlorophyll b. Parallels between these properties and those found in in-vivo systems may help to find models for the chlorophyll configurations occuring in in-vivo systems.

A molecule in its metastable triplet state can be characterized by static and by kinetic parameters. The static parameters are the so-called fine-structure constants $D$ and $E$, which describe the splitting of the state in zero field due to the dipolar interaction of the two unpaired electrons, (see Fig. 1A). If one designates the $z$-axis as the axis perpendicular to the plane of the chlorophyll molecule (Fig. 1B) and the $x$ and $y$-axes in the plane of the molecule, the bottom zero field level for these flat "pancake-like" molecules is the spin state $t_z$ (a state in which the spin moves in the $xy$-plane). The two top levels can be assigned to the spin states $t_x$ and $t_y$, which are defined correspondingly. The splitting between these states is indicated in Fig. 1A and can be used to define the fine structure constants. The kinetic constants are the rate constants for the population and depopulation of the zero-field levels which are relevant in the excitation and deexcitation cycle shown in Fig. 1A, [26, 27]. To describe the full dynamic behaviour spin lattice relaxation processes between the spin levels may be important. The rate constants for such processes connecting the levels $t_i$ and $t_j$ will be designated as $w_{ij}$ in the following. In principal it is possible to derive these static and kinetic constants from the static and dynamical behaviour of the ESR spectra.

Since these molecular parameters depend critically on the interaction with the environment, they

Reprint requests to Prof. Dr. H. C. Wolf, Physikalisches Institut, Teil 3, Universität Stuttgart, Pfaffenwaldring 57, D-7000 Stuttgart 80.

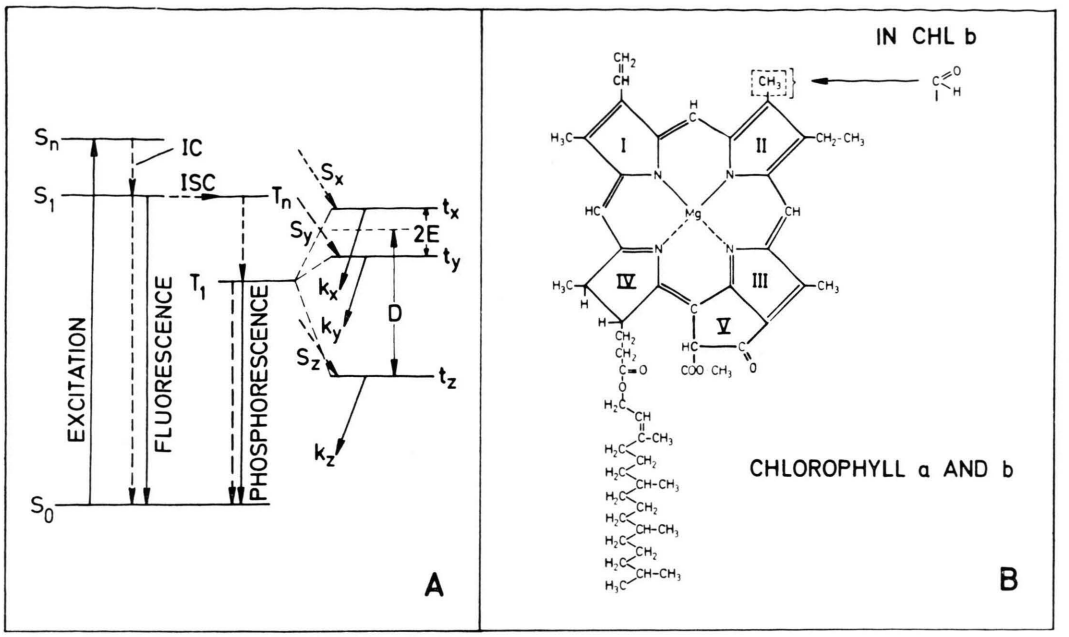


Fig. 1. A) Schematic representation of the relevant energy levels and transitions during the excitation — deexcitation cycle in the experiments of this work. Full lines indicate radiative transitions, broken lines radiationless transitions. The left hand part illustrates the electronic transitions between the groundstate and the singlet and triplet excited states; the right hand part defines in an enlarged scale the rate constants for the selective population and depopulation of the triplet sublevels $t_x$, $t_y$ and $t_z$. $S_0$, $S_1$, $S_n$: singlet states, $T_1$, $T_n$: triplet states; s: rate constants for population, k: rate constants for depopulation; D, E: finestructure constants; IC: internal conversion; ISC: intersystem crossing. B) Structure of chlorophyll a and chlorophyll b. The molecular $z$-axis is perpendicular to the plane of the molecule, $x$ and $y$ are in plane.

can reflect the interaction of a chlorophyll molecule either with solvent molecules or with another chlorophyll molecule in a dimer arrangement. Such "special dimers" in their triplet state play a crucial role in the "upconversion model" by Fong [24].

It is the aim of this work to study the concentration dependence of these molecular parameters and to try to extract information about the complex formation behaviour of chlorophyll. Furthermore, we attempt to apply this technique to in-vivo systems. We will reinterpret the experimental results on bacteriochlorophyll by Clarke and coworkers [9, 14] and propose a tentative model for such a dimer in vivo as well as for dimeric forms of chlorophyll b in vitro.

## 2. Experimental

### *2.1. Sample Preparation*

Chlorophyll a and b was purchased from Sigma Chemical Company (product No. C-5753 and C-5878, respectively). To get rid of residual water all chlorophyll was dried carefully by dissolving it several times in waterfree methanol which was subsequently pumped off until a solvent vapor pressure of $10^{-4}$ to $10^{-5}$ Torr was reached. The dried chlorophylls were dissolved at concentrations of $1.5 \times 10^{-5}$ to $1 \times 10^{-3}$ mole/l in methylmethacrylate (MMA, Röhm and Haas) and of $10^{-6}$ to $10^{-1}$ mole/l in methyltetrahydrofurane (MTHF, Merck-Schuchardt), which had been purified by repeated chromatography and vacuum destillation. Following a repeated degassing cycle the MTHF samples were sealed in a quartz sample tube, whereas the MMA was polymerized to PMMA by adding the catalyzer Porofor N (Bayer) at a concentration of $10^{-3}$ mole/l.

### *2.2. Instrumental*

Figure 2 presents a block diagram of the entire ESR setup. Since all experiments were done at liquid helium temperature the sample had to be immersed in a cryostat. This cryostat has been described previously [28].

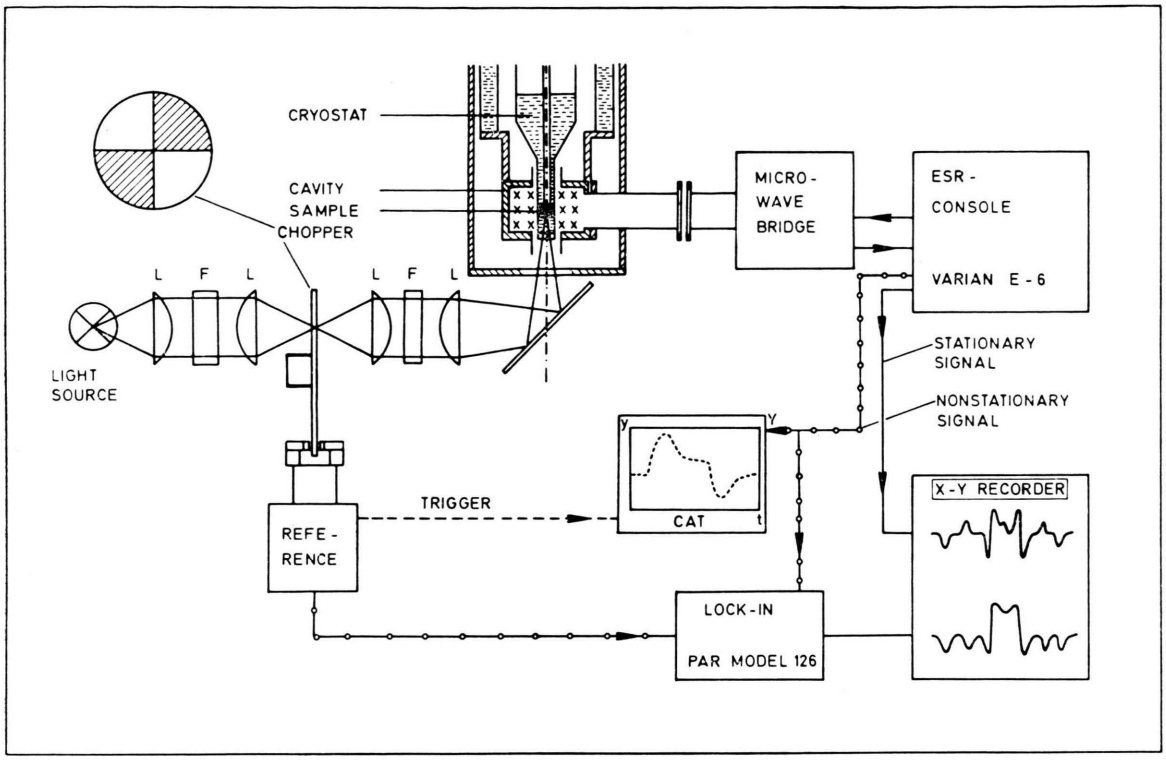


Fig. 2. Block diagram. Conventional ESR can be recorded using a Varian E-6 spectrometer. The light originates from a high pressure xenon arc (XBO 450 W/2, Osram). It is passed through appropriate filters F and lenses L and focussed onto the sample. For the nonstationary spectra it is chopped using a rotating disk. The reference signal for the double lock-in technique and the CAT is obtained from a photodiode which monitors a chopped reference light.

Optical excitation in the wavelength region between 400 and 700 nm was achieved using a xenon high-pressure arc (XBO 450 W/2, Osram) and suitable filters (GG3 (5 mm) + KG3 (2 mm), Schott, + edge filter $\lambda < 700$ nm, Coherent Radiation + water (7 cm)).

The ESR spectra were recorded using a commercial spectrometer with 100-kHz field modulation (model E-6, Varian). Apart from performing conventional ESR experiments in many cases the light was chopped additionally (chopping frequency between 0.25 and 2000 Hz) in order to improve the signal to noise ratio and to obtain additional information about the kinetic parameters. In these experiments either a double lock-in technique (both at the field-modulation and the chopping frequency) could be used, thus eliminating the light-independent stationary ESR signals, or the kinetic behaviour of the ESR signal amplitude after switching the light on or off could be studied. In the latter case the output of the 100-kHz lock-in amplifier was recorded using a signal averager (model 5480, Hewlett Packard).

Qualitative information about the dynamic behaviour of the ESR signals may also be obtained by studying the way the double lock-in signal depends on the chopping frequency. This is illustrated qualitatively in Figure 3. Three different cases of the kinetic behaviour are distinguished in this illustration:

A) a monotonous approach of a purely absorptive signal to its equilibrium level after the light is switched on or off suddenly,
B) an absorptive signal which overshoots its equilibrium value after the sudden switching of the light,
C) an emissive ESR signal with an absorptive overshooting after the light is switched on.

All three cases have been observed in molecular crystals [26, 27]. The accompanying ESR signals depend differently on a variation of the chopping

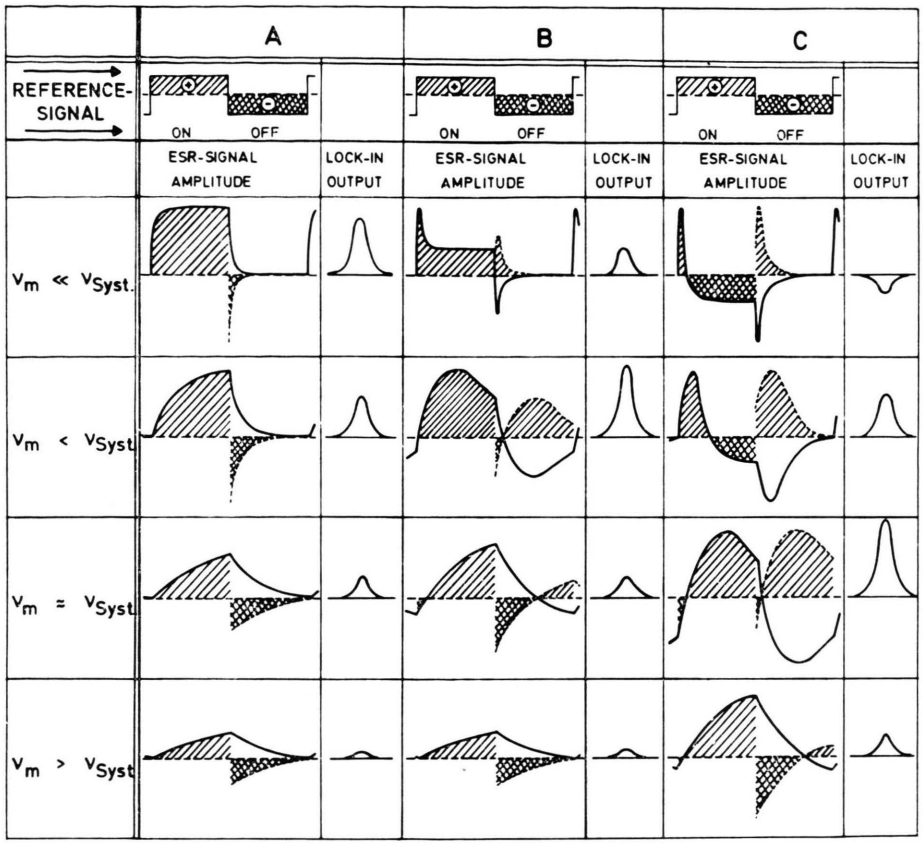


Fig. 3. Qualitative behaviour of the ESR-signal amplitudes at chopped excitation using double lock-in techniques for various experimental parameters. See text for detailed explanation.
A) Stationary absorptive signal without overshooting,
B) stationary absorptive signal with absorptive overshooting,
C) stationary emissive signal with absorptive overshooting.

frequency. In case A the signal amplitude drops monotonously, if the chopping frequency is raised from low values to values which are high compared to the inverse of the systems characteristic time constant. In case B the lock-in signal reaches a maximum value, if the chopping frequency equals the inverse time constant, whereas in case C it reverses its sign when passing through the critical chopping frequency.

In this way it was possible to estimate the system's rate constants by looking at the chopping-frequency dependence of the double lock-in signal.

## 3. Experimental Results

### *3.1. ESR Spectra*

Figure 4 shows the ESR spectra obtained from chlorophyll a molecules in a matrix of PMMA at various concentrations ($1.5 \times 10^{-5}$, $2 \times 10^{-4}$ and $8 \times 10^{-4}$ mole/l). They were obtained using the double lock-in technique described in section 2.2. Since the molecules are oriented at random the sample yields the familiar "glass-spectrum" pattern, which has been discussed in great detail by Kottis [29]. He has shown that the lines observed in the differentiated ESR spectra at the field strengths labelled $B_x^{\pm}$, $B_y^{\pm}$ and $B_z^{\pm}$ result from the low and the high field transition ($m_s = 0 \leftrightarrow m_s = \pm 1$) of molecules in canonical orientations ($B_0$ parallel $x$, $y$ and $z$, respectively). Thus the fine-structure constants may be obtained from these spectra in a first-order approximation using the well known relations

$$D = \tfrac{1}{2} g_z \mu_B (B_z^+ - B_z^-), \tag{1a}$$

$$D + 3E = g_x \mu_B (B_x^+ - B_x^-), \tag{1b}$$

$$D - 3E = g_y \mu_B (B_y^+ - B_y^-). \tag{1c}$$

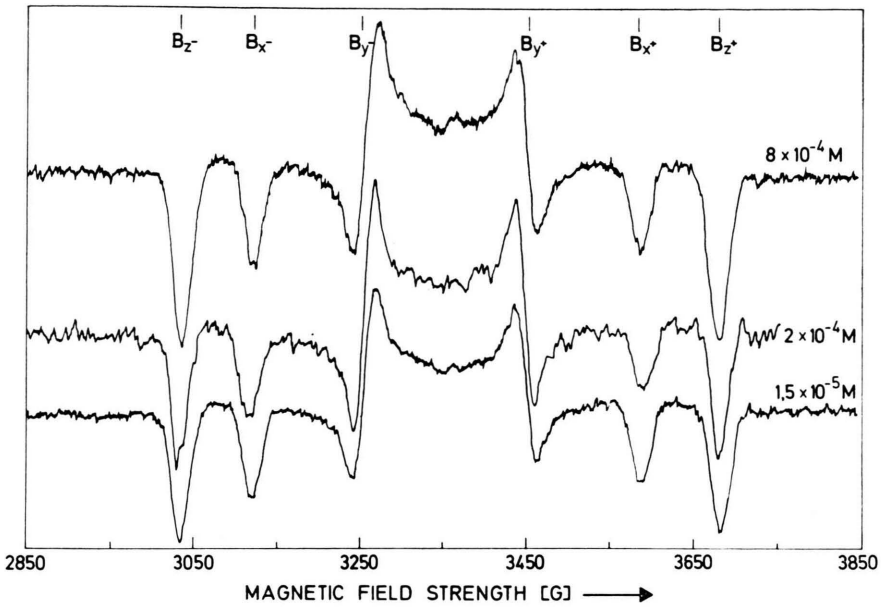


Fig. 4. ESR-spectra of chlorophyll a in PMMA at 4.2 K. Concentrations: $8 \times 10^{-4}$, $2 \times 10^{-4}$ and $1.5 \times 10^{-4}$ mole/l. Light-chopping frequency: 50 Hz.

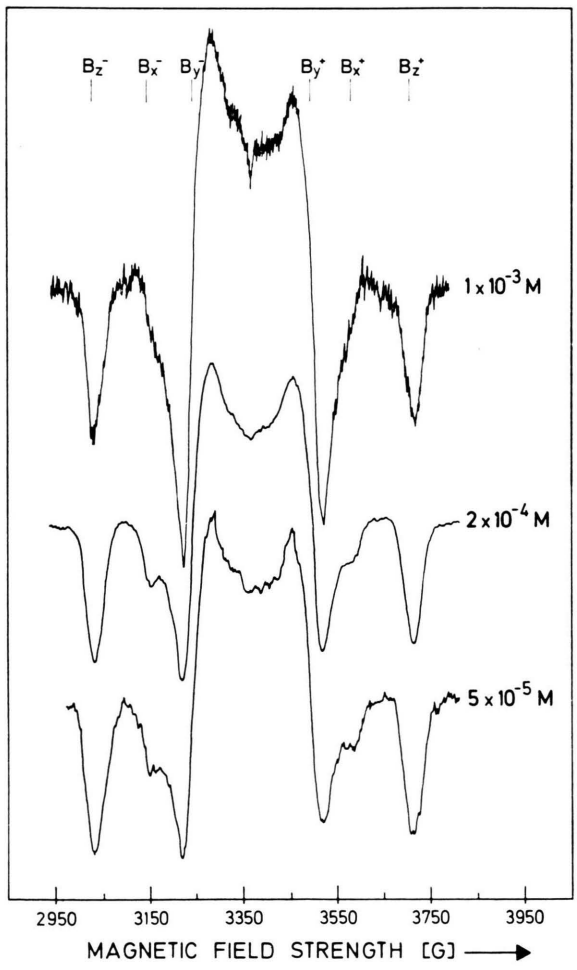


Assuming $g_x = g_y = g_z \approx 2$, this yields for the fine-structure constants of chl a in PMMA in the covered range of concentration (low concentration, species AO):

$$\text{(AO)}: \quad D = (303 \pm 3) \times 10^{-4}\ \text{cm}^{-1},$$
$$E = (42 \pm 3) \times 10^{-4}\ \text{cm}^{-1}.$$

Figure 5 shows analogous spectra for chl b in PMMA ($c = 5 \times 10^{-5}, 2 \times 10^{-4}$ and $1 \times 10^{-3}$ mole/1). They can be interpreted by using the following numbers for the fine-structure constants of chl b in PMMA in the low concentration limit:

$$\text{(BO)}: \quad D = (320 \pm 5 \times 10^{-4}\ \text{cm}^{-1},$$
$$E = (32 \pm 3) \times 10^{-4}.$$

However, there is an indication that the observed spectra for $10^{-3}$ mole/l result from a superposition of two different species with slightly different fine-structure constants ($D = (314 \pm 3) \times 10^{-4}\ \text{cm}^{-1}$, $E = (29 \pm 3) \times 10^{-4}\ \text{cm}^{-1}$ and $D = (323 \pm 3) \times 10^{-4}\ \text{cm}^{-1}$, $E = (34 \pm 3) \times 10^{-4}\ \text{cm}^{-1}$, respectively) and different rate constants. This presumption is hinted by a slight shift of the observed line positions, if the response time of the low-frequency lock-in amplifier (light-chopping frequency) is varied. It is also hinted by a very small splitting

Fig. 5. ESR-spectra of chlorophyll b in PMMA at 4.2 K. Concentrations: $1 \times 10^{-3}$, $2 \times 10^{-4}$ and $5 \times 10^{-5}$ mole/l. Light-chopping frequency: 50 Hz.

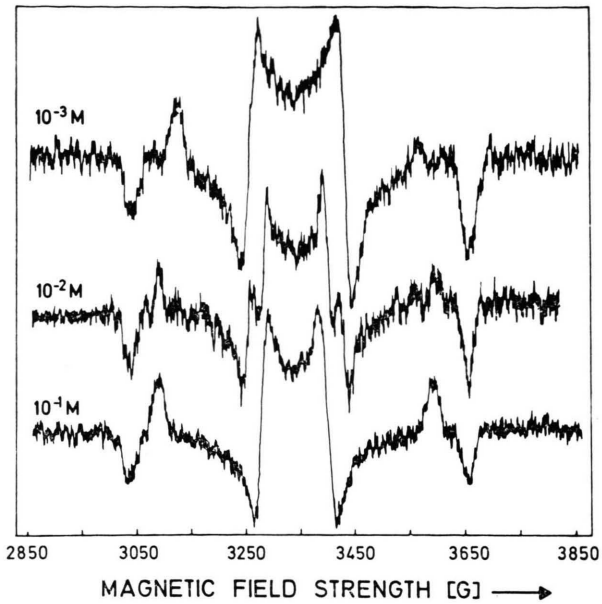


Fig. 6. ESR-spectra of chlorophyll a in MTHF at 4.2 K. Concentrations: $10^{-3}$, $10^{-2}$ and $10^{-1}$ mole/l. Light-chopping frequency: 110 Hz.

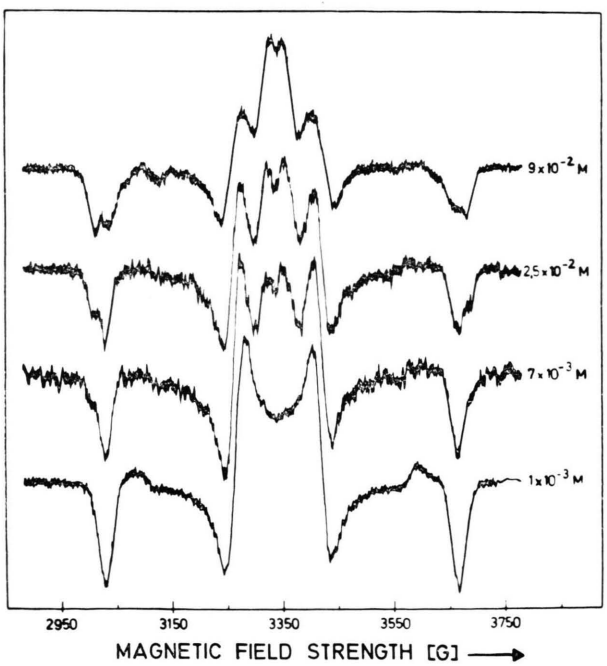


Fig. 7. ESR-spectra of chlorophyll b in MTHF at 4.2 K. Concentrations: $9 \times 10^{-2}$, $2.5 \times 10^{-2}$, $7 \times 10^{-3}$ and $1 \times 10^{-3}$ mole/l. Light-chopping frequency: 40 Hz.

of some of the lines observed in the spectra with continuous excitation (see for example Fig. 9, $B_z^{\pm}$).

Compared to the spectra of a system of triplet-state molecules at random orientations in thermal equilibrium as discussed by Kottis [29] some of the lines have reversed signs. This is due to the well known spin polarization occuring in the singlet $\leftrightarrow$ triplet transition [26, 27, 30]. As has been mentioned before (Sect. 2.2) this can be used to estimate the rate constants for the population and depopulation of the zero-field sublevels of the triplet state. We will discuss this in detail in the following section.

Figures 6 and 7 present the respective ESR spectra for chl a and chl b in MTHF at various concentrations. In these spectra a significant influence of the chlorophyll concentration is observed. For instance the spectrum from $10^{-3}$ mole/l chlorophyll a in MTHF yields the following fine-structure constants:

$$(A1): \quad D = (288 \pm 3) \times 10^{-4}\,\mathrm{cm}^{-1}, \quad E = (42 \pm 3) \times 10^{-4}\,\mathrm{cm}^{-1}.$$

If the concentration of chl a is increased to $10^{-2}$ or $10^{-1}$ mole/l another set of fine-structure constants accounts for the observed spectra:

$$(A2): \quad D = (291 \pm 3) \times 10^{-4}\,\mathrm{cm}^{-1}, \quad E = (59 \pm 3) \times 10^{-4}\,\mathrm{cm}^{-1}.$$

For chlorophyll b in MTHF the observed concentration dependence is more complicated:

At low concentrations ($\leqq 10^{-3}$ mole/l) the observed fine-structure constant are

$$(B1): \quad D = (294 \pm 3) \times 10^{-4}\,\mathrm{cm}^{-1}, \quad E = (49 \pm 3) \times 10^{-4}\,\mathrm{cm}^{-1}.$$

If the concentration is increased to $10^{-2}$ mole/l, the additional spectra can be explained using

$$(B2): \quad D = (315 \pm 3) \times 10^{-4}\,\mathrm{cm}^{-1}, \quad E = (87 \pm 3) \times 10^{-4}\,\mathrm{cm}^{-1}.$$

Following a further increase of the concentration the chl b spectra become quite complicated and must be attributed to a superposition of different triplet spectra. By varying the light-chopping frequency between 0.25 and 2000 Hz systematically it was possible to identify three additional triplet species in order to account for the observed spectra:

$$(B3): \quad D = (325 \pm 5) \times 10^{-4}\,\mathrm{cm}^{-1}, \quad E = (29 \pm 5) \times 10^{-4}\,\mathrm{cm}^{-1},$$

$$(B4): \quad D = (272 \pm 3) \times 10^{-4}\,\mathrm{cm}^{-1}, \quad E = (41 \pm 3) \times 10^{-4}\,\mathrm{cm}^{-1},$$

$$(B5): \quad D = (255 \pm 3) \times 10^{-4}\,\mathrm{cm}^{-1}, \quad E = (69 \pm 3) \times 10^{-4}\,\mathrm{cm}^{-1}.$$

This assignement was made possible by observing the following simple relation, which we will call the triplet resonance-field identity, and which can be easily derived from the spin Hamiltonian of the triplet state [31]. It states that for a given triplet system the resonance fields observed in the glass spectrum must obey the simple relation

$$\left(\frac{B_x^-}{B_x^+}\right)^2 \cdot \left(\frac{B_y^-}{B_y^+}\right)^2 \cdot \left(\frac{B_z^+}{B_z^-}\right)^2 = 1\,. \qquad (2)$$

It is straightforward to prove this statement generally, even for anisotropic g factors, simply by calculating the resonance field strengths for the canonical orientations [32] and multiplying them in the indicated fashion. The triplet resonance-field identity is quite useful to determine whether the assignement of a set of ESR-lines in a complicated glass spectrum to one particular triplet species is adequate or not.

Table 1 summarizes the triplet species observed in the different samples and their respective fine-structure constants.

Table 1. Fine-structure constants of chl a and chl b in PMMA and MTHF at various concentrations.

| Matrix | Molecule | Concentration [mole/l] | Fine-structure constants [$10^{-4}$ cm$^{-1}$] $D$ | E | Symbolic Labelling |
|---|---|---|---|---|---|
| PMMA | Chl a | $10^{-5} - 10^{-3}$ | $303 \pm 3$ | $42 \pm 3$ | A0 |
| | Chl b | $10^{-5} - 10^{-3}$ | $320 \pm 5$ | $32 \pm 3$ | B0 |
| MTHF | Chl a | $10^{-3}$ | $288 \pm 3$ | $42 \pm 3$ | A1 |
| | Chl a | $10^{-2}$ | $288 \pm 3$ | $42 \pm 3$ | A1 |
| | | | $291 \pm 3$ | $59 \pm 3$ | A2 |
| | Chl a | $10^{-1}$ | $291 \pm 3$ | $59 \pm 3$ | A2 |
| | Chl b | $10^{-4}$ | $294 \pm 3$ | $49 \pm 3$ | B1 |
| | Chl b | $2.5 \times 10^{-2}$ | $294 \pm 3$ | $49 \pm 3$ | B1 |
| | | | $315 \pm 3$ | $87 \pm 3$ | B2 |
| | Chl b | $10^{-1}$ | $294 \pm 3$ | $49 \pm 3$ | B1 |
| | | | $315 \pm 3$ | $87 \pm 3$ | B2 |
| | | | $325 \pm 5$ | $29 \pm 5$ | B3 |
| | | | $272 \pm 3$ | $41 \pm 3$ | B4 |
| | | | $255 \pm 3$ | $69 \pm 3$ | B5 |

### *3.2. Optical Electronspin Polarization (OEP)*

It was mentioned in the previous sections that some of the observed ESR transitions are emissive (Sect. 3.1) and that in such cases the size and even the sign depends on the choice of the light-chopping frequency relative to the characteristic time constants of the system (Sect. 2.2). As an example Fig. 8 (lower curve) shows the spectrum obtained from chl a in PMMA ($2 \times 10^{-4}$ mole/l) at continuous excitation. Comparing this spectrum with the pattern given by Kottis [29] for a purely absorptive system it is obvious that some of the lines are absorptive ($A$) and some are emissive ($E$):

$$B_z^-: E/B_x^-: A/B_y^-: E;\ B_y^+: A/B_x^+: E/B_z^+: A\,.$$

From this pattern the following inequality for the relative occupation numbers of the spin levels can be deduced [33]

$$N_y > N_x\,,\ N_z\,.$$

The influence of nonstationary effects in the chopped-excitation spectra is demonstrated by the comparison of this pattern with the upper curve in Figure 8. In the latter case the light was chopped at a frequency of 50 Hz, and it is clearly seen that the lines at $B_x^{\pm}$ have reversed their signs. This observation manifests an emissive overshooting of this line after switching on the light as discussed in Section 2.2. This yields for the occupation numbers immediately after switching on the light $N_x, N_y > N_z$.

Figure 9 illustrates the corresponding spectra for chl b in PMMA. Whereas in the chopped spectra all three low-field lines are emissive and the high-field lines are absorptive indicating a occupation $N_x$, $N_y > N_z$, the lines at $B_y^-$ and $B_y^+$ in the steady-state spectra have reversed their signs compared to the

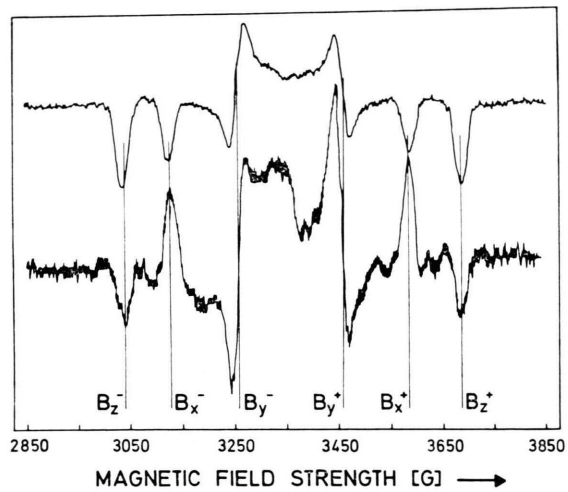


Fig. 8. Comparison of the light-chopped ESR signal (top) of chl a in PMMA ($2 \times 10^{-4}$ mole/l, 50 Hz) to the stationary signal of the same sample (bottom).

Table 2. Stationary and nonstationary OEP patterns and triplet-level occupation numbers.

| Molecule/ Matrix | Stationary OEP | | | | | | | Nonstationary OEP | | | | | | |
|---|---|---|---|---|---|---|---|---|---|---|---|---|---|---|
| | Character of ESR line ($E$ = emissive $A$ = absorptive) | | | | | | Occupation numbers | Character of ESR line ($E$ = emissive $A$ = absorptive) | | | | | | Occupation numbers |
| | $B_z^-$ | $B_x^-$ | $B_y^-$ | $B_y^+$ | $B_x^+$ | $B_z^+$ | | $B_z^-$ | $B_x^-$ | $B_y^-$ | $B_y^+$ | $B_x^+$ | $B_z^+$ | |
| Chl a/PMMA | E | A | E | A | E | A | $N_y > N_x, N_z$ | E | E | E | A | A | A | $N_x, N_y > N_z$ |
| Chl b/PMMA | E | E | A | E | A | A | $N_x > N_y, N_z$ | E | E | E | A | A | A | $N_x, N_y > N_z$ |
| Chl a/MTHF | E | A | E | A | E | A | $N_y > N_x, N_z$ | E | A | E | A | E | A | $N_y > N_x, N_z$ |
| Chl b/MTHF | E | E | A | E | A | A | $N_x > N_y, N_z$ | E | (E) | E | A | (A) | A | $N_x, N_y > N_z$ |

chopped spectra indicating a initial occupation $N_x > N_y, N_z$.

In a similar way both the stationary and the nonstationary OEP for chl a and chl b in MTHF can be analyzed. It turns out that these qualitative results in both matrices do not depend on the concentration. The results are compiled in Table 2.

Chlorophyll a exhibits in both matrices the same stationary pattern, but in the nonstationary case $B_x^-$ is emissive in PMMA and $B_x^+$ absorptive whereas in MTHF $B_x^-$ is absorptive and $B_x^+$ emissive. For chlorophyll b both the stationary and the nonstationary patterns agree in both matrices qualitatively with each other. However for chl a/MTHF our pattern does not agree with that observed by Kleibeuker et al. [20]. They observed a nonstationary polarization pattern of the type E, E, A/E, A, A. This discrepancy is not yet understood.

### *3.3. Kinetic Rate Constants*

The time dependence of the ESR signal intensity following a sudden switching of the excitation light is determined by the rate constants for the population and depopulation, $s_i$ and $k_i$ respectively, of the Zeeman level $|t_i\rangle$ ($i = 0$ or $\pm 1$), and by the spin lattice relaxation rates indicated in Figure 10. For convenience we have abbreviated the latter quantities. $w_1$ is an abbreviation for the relaxation rate from $|t_1\rangle$ to $|t_0\rangle$, $w_1 = w_{1,0}$. $w_2$ and $w_3$ are defined similarly: $w_2 = w_{0,-1}$, $w_3 = w_{1,-1}$. $e_1$, $e_2$ and $e_3$ are abbreviations for the Boltzmann factors of these pairs of Zeeman levels. $b_1$, $b_{-1}$ and $b_0$ are the corresponding microwave transition probabilities. The rate constants $s_i$ and $k_i$ are related to the zero-field rates in the well known way [27].

It is straight forward to write down the rate equations for the occupation numbers of the Zeeman levels of the system illustrated in the right hand part of Figure 10. The solution of these equations is facilitated by assuming that the ratio of the population numbers of $|t_{+1}\rangle$ and $|t_{-1}\rangle$ is $N_1/N_{-1} \approx e_3$, independent of the degree of spin polarization. This assumption is justified in first order approximation for $X$-Band experiments, since $N_1/N_{-1}$ in this case can vary only between $e_3 \approx 0.82$ (thermal equilibrium) and 1 (complete spin polarization). Using this approximation the rate equations are:

$$\begin{aligned}\dot{N}_0 = &-(k_0 + w_1 e_1 + w_2 + s_0 + b_1 + b_{-1}) N_0 \\ &+ (w_1 e_3 + w_2 e_2 - s_0(1 + e_3) \\ &+ b_1 e_3 + b_{-1}) N_{-1} + s_0 N\,, \end{aligned} \tag{3a}$$

$$\begin{aligned}\dot{N}_{-1} = &(w_2 - s_1 + b_{-1}) N_0 \\ &- [k_1 + w_2 e_2 + b_{-1} + s_1(1 + e_3)] N_{-1} + s_1 N\,, \end{aligned} \tag{3b}$$

$$\dot{N}_1 = e_3 \dot{N}_{-1}; \quad N_1 = e_3 N_{-1}\,. \tag{3c}$$

$N$ is the total number of chlorophyll molecules. The $s_i$ account for the transition probabilities from the singlet ground state to the excited singlet states multiplied with the fraction of excited molecules which crosses over to the state $|t_i\rangle$. $b_0$ was neglected in writing down Eqs. (3), since ($\Delta m = 2$)-transitions are negligible in the experiments under consideration. In the following we will neglect all the microwave-induced transition rates, since all experiments were performed at microwave levels far below saturation.

The coupled differential equations (3) can be solved readily yielding for the time dependence of the occupation numbers a superposition of two exponential approaches to the equilibirum value:

$$N_0 = N_0^{(0)} + N_0^{(1)} e^{-r_1 t} + N_0^{(2)} e^{-r_2 t}\,, \tag{4a}$$

$$N_{-1} = N_{-1}^{(0)} + N_{-1}^{(1)} e^{-r_1 t} + N_{-1}^{(2)} e^{-r_2 t}\,, \tag{4b}$$

$$N_1 = e_3 N_{-1} \tag{4c}$$

$r_1$ and $r_2$ are the roots of the secular determinant

$$\begin{vmatrix} -[k_0 + w_1 e_1 + w_2 + s_0 - r] & [w_1 e_3 + w_2 e_2 - s_0(1 + e_3)] \\ [w_2 - s_1] & -[k_1 + w_2 e_2 + s_1(1 + e_3) - r] \end{vmatrix} = 0 . \tag{5}$$

It should be remembered that Eq. (5) depends on the orientation of the magnetic field with respect to the molecular principal axes frame, since the high-field rate constants depend on the orientation. For instance, for $B_0$ parallel to $x$ the rate constants are given by $k_0 = k_x$ and $k_1 = k_{-1} = \frac{1}{2}(k_y + k_z)$. Analogous relations hold for the other canonical orientations [27].

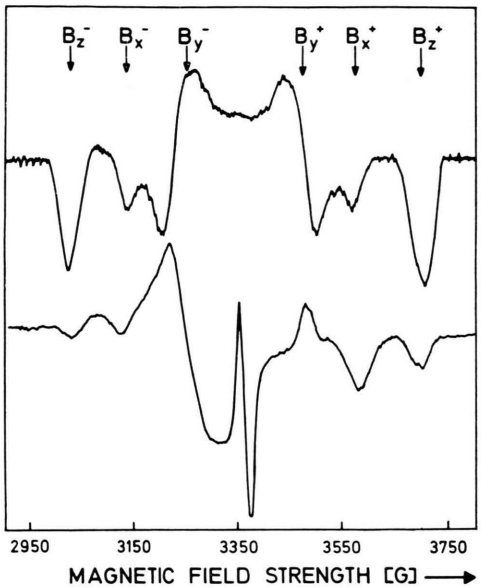


Fig. 9. Comparison of the light-chopped ESR signal (top) of chl b in PMMA ($1.5 \times 10^{-3}$ mole/l, 50 Hz) to the stationary signal of the same sample (bottom).

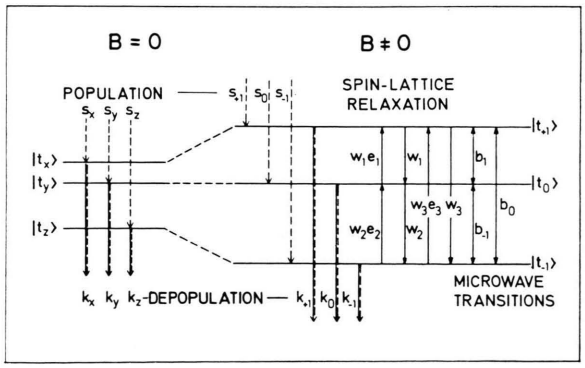


Fig. 10. Rate constants for population and depopulation of the triplet-state sublevels in zero field and in high field together with microwave and spin-lattice transition probabilities.

Since the ESR signals are proportional to the difference of the occupation numbers of the levels envolved, they are proportional to a superposition of the same exponentials and their time dependence reflects the rate constants $r_1$ and $r_2$ obtained from Equation (5).

Figure 11 presents examples for this time dependence of the ESR signals obtained from chl b in MTHF ($10^{-4}$ mole/l). The ESR signal for each canonical orientation approaches its new equilibrium value in agreement with the predictions of Eqs. (4) after the light is switches on or off suddenly. Thus we can determine the roots of the secular equation (5) for the canonical orientations experimentally.

In order to relate these experimentally determined quantities to the rate constants let us consider first the turn-off process ($s_1 = s_0 = 0$). For this

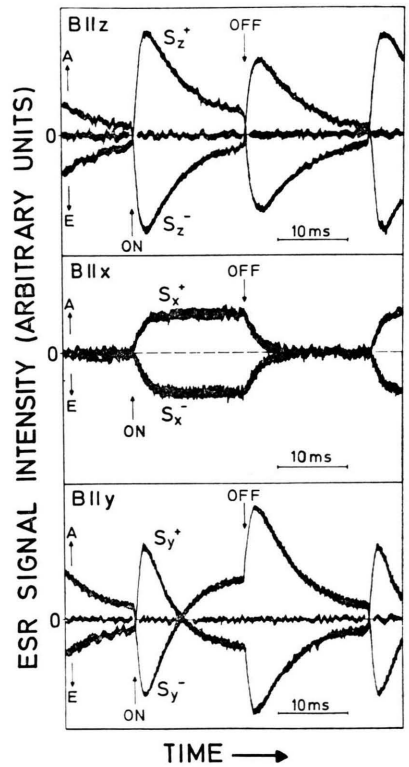


Fig. 11. Kinetics of ESR-signal amplitudes of chlorophyll b in MTHF ($10^{-4}$ mole/l) for the high-field and low-field transitions of molecules in the canonical orientations.

Table 3. Rate constants for the population and depopulation of triplet states of chl a and chl b in PMMA and MTHF.

| System | Depopulation rate constants [$s^{-1}$] | | | | Spin lattice relaxation rate constants [$s^{-1}$] | | | Population rates |
|---|---|---|---|---|---|---|---|---|
| | $k_T$ | $k_x$ | $k_y$ | $k_z$ | $w_x$ | $w_y$ | $w_z$ | $s_x$, $s_y$, $s_z$ |
| *Chl a in PMMA* (AO) | $270 \pm 30$ | $420 \pm 30$ | $355 \pm 30$ | $25 \pm 10$ | $80 \pm 40$ | $130 \pm 50$ | $50 \pm 40$ | $s_x \approx s_y > s_z$ |
| *Chl b in PMMA* (BO) | $220 \pm 30$ | $420 \pm 40$ | $220 \pm 30$ | $20 \pm 15$ | $110 \pm 60$ | $200 \pm 60$ | $190 \pm 50$ | $s_x \approx s_y > s_z$ |
| *Chl a in MTHF* | | | | | | | | |
| A1 ($10^{-3}$ M/l) | $460 \pm 50$ | $310 \pm 40$ | $930 \pm 90$ | $150 \pm 25$ | $750 \pm 120$ | $250 \pm 110$ | $150 \pm 90$ | $s_y > s_x > s_z$ |
| A2 ($10^{-1}$ M/l) | $730 \pm 80$ | $1180 \pm 120$ | $830 \pm 80$ | $180 \pm 30$ | $20_{(\pm)}150$ | $220 \pm 140$ | $200 \pm 130$ | $s_y > s_x > s_z$ |
| *Chl b in MTHF* | | | | | | | | |
| B1 ($10^{-4}$ M/l) | $200 \pm 30$ | $195 \pm 30$ | $380 \pm 40$ | $20 \pm 10$ | $125 \pm 50$ | $265 \pm 60$ | $285 \pm 60$ | $s_x \approx s_y > s_z$ |

discussion we will furthermore use the approximation $e_1 = e_2 = \sqrt{e_3} = e \approx 0.9$ and $w_1 = w_2 = w$. Vieta's formula for the roots $r^i_{A,1}$ and $r^i_{A,2}$ of the quadratic eq. (5) yields

$$r^i_{A1} + r^i_{A2} = k^i_0 + k^i_1 + (1 + 2e)\, w^i\,, \tag{6a}$$

$$r^i_{A1} \times r^i_{A2} = k^i_0 k^i_1 + ((1 + e)\, k^i_1 + e\, k^i_0)\, w^i\,. \tag{6b}$$

The index $A$ designates the turn-off process, the superscript $i$ stands for the canonical orientation $x$, $y$ or $z$. Equations (6) yield a quadratic equation for $k^i$. Substituting $e = 0.9$ into this equations gives finally

$$\begin{aligned} k^{\pm}_i = {} & 1.0364\, k_T - 0.0182\, (r^i_{A1} + r^i_{A2}) \\ & \pm [-2.2612\, k^2_T + 2.0350\, (r^i_{A1} + r^i_{A2})\, k_T \\ & - 2.0364\, r^i_{A1} r^i_{A2} + 0.0003\, (r^i_{A1} + r^i_{A2})^2]^{1/2}\,. \end{aligned} \tag{7}$$

$k_T$ is the inverse triplet lifetime:

$$k_T = \tfrac{1}{3}\,(k_x + k_y + k_z) = \tfrac{1}{3}\,(2\,k^i_1 + k_0)\,. \tag{8}$$

The three Eqs. (7) are double valued yielding eight arithmetically possible combinations. However, Eq. (8) allows in general to rule out at least six of these combinations. The final ambiguity can then be removed by consulting the qualitative results of Section 3.2. Substituting these numbers for $k^i$ into Eq. (6a) the spin lattice relaxation rates $w_i$ can be obtained. In principal it is possible to determine also the rate constants for the population, $s^i$, from the approach to the equilibrium after switching on the light. However, the experimental errors were too large to allow a determination of the absolute numbers. Thus only their relative size could be determined. Table 3 summarizes the rate constants obtained by this procedure for various systems.

Corresponding results on chl a and chl b in various matrices have been published by Clarke and coworkers [22] and by Kleibeuker et al. [34]. The rate constant reported in this work are in general approximately 30% lower than the previous numbers. A reason for this difference is not known. Apart from this systematic discrepancy, however, there is good qualitative agreement between the various results. In particular in all cases both the population and the depopulation of the cholrophyll triplet levels occurs preferentially via the spin levels $|t_x\rangle$ and $|t_y\rangle$. A detailed discussion of the intersystem crossing rates using existing theoretical concepts is not yet possible because the chlorophyll molecules are too complex. Attempts in this direction have been performed by Clarke and coworkers [22] on a wider background of experimental results (chlorophyll and related compounds).

*Acknowledgements*

The authors are sincerely grateful to F. Drissler for many valuable suggestions concerning both the realization of the experiments and their interpretation. Helpful discussions with Dr. H. Sixl are also gratefully acknowledged.

[1] P. L. Dutton, J. S. Leigh, and M. Seibert, Biochem. Biophys. Res. Commun. **46**, 406 (1972).
[2] P. L. Dutton, J. S. Leigh, and D. W. Reed, J. Amer. Chem. Soc. **94**, 7197 (1972).
[3] P. L. Dutton, J. S. Leigh, and D. W. Reed, Biochim. Biophys. Acta **292**, 654 (1973).
[4] C. A. Wraight, J. S. Leigh, P. L. Dutton, and R. K. Clayton, Biochim. Biophys. Acta **333**, 401 (1974).
[5] R. A. Uphaus, J. R. Norris, and J. J. Katz, Biochem. Biophys. Res. Commun. **61**, 1057 (1974).
[6] R. H. Clarke and R. H. Hofeldt, J. Chem. Phys. **61**, 4582 (1974).

[7] R. H. Clarke and R. E. Connors, Chem. Phys. Letters **33**, 365 (1975).
[8] R. H. Clarke, R. E. Connors, J. R. Norris, and M. C. Thurnauer, J. Amer. Chem. Soc. **97**, 7178 (1975).
[9] R. H. Clarke, R. E. Connors, and H. A. Frank, Biochem. Biophys. Res. Commun. **71**, 671 (1976).
[10] R. H. Clarke and R. E. Connors, Chem. Phys. Letters **42**, 69 (1976).
[11] A. J. Hoff and J. H. van der Waals, Biochim. Biophys. Acta **423**, 615 (1976).
[12] A. J. Hoff, Biochim. Biophys. Acta **440**, 765 (1976).
[13] M. C. Thurnauer and J. R. Norris, Chem. Phys. Letters **47**, 100 (1977).
[14] R. H. Clarke, R. E. Connors, H. A. Frank, and J. C. Hoch, Chem. Phys. Letters **45**, 523 (1977).
[15] J. M. Lhoste, C. R. Acad. Sci. Paris **266**D, 1059 (1968).
[16] H. Levanon and A. Scherz, Chem. Phys. Letters **31**, 119 (1975).
[17] J. F. Kleibeuker and T. J. Schaafsma, Chem. Phys. Letters **29**, 116 (1974).
[18] J. R. Norris, H. Scheer, and J. J. Katz, Ann. New York Acad. Sci. **244**, 260 (1975).
[19] J. R. Norris, R. A. Uphaus, and J. J. Katz, Chem Phys. Letters **31**, 157 (1975).
[20] J. F. Kleibeuker, R. J. Platenkamp, and T. J. Schaafsma, Chem. Phys. Letters **41**, 557 (1976).
[21] S. J. van der Bent, T. J. Schaafsma, and J. C. Goodheer, Biochem. Biophys. Res. Commun. **71**, 1147 (1976).
[22] R. H. Clarke, R. E. Connors, T. J. Schaafsma, J. F. Kleinbeuker, and R. J. Platenkamp, J. Amer. Chem. Soc. **98**, 3674 (1976).
[23] J. J. Katz and J. R. Norris, Current Topics Bioenerg. **5**, 41 (1973).
[24] F. K. Fong, Appl. Phys. **6**, 151 (1975).
[25] H. Chow, R. Serlin, and C. E. Strouse, J. Amer. Chem. Soc. **97**, 7230 (1975).
[26] M. Schwoerer and H. Sixl, Z. Naturforsch. **24a**, 952 (1969).
[27] H. Sixl and M. Schwoerer, Z. Naturforsch. **25a**, 1383 (1970).
[28] M. Schwoerer and H. C. Wolf, Mol. Cryst. **3**, 177 (1967).
[29] P. Kottis, Ann. Phys. Paris **4**, 459 (1969).
[30] J. H. van der Waals and M. S. de Groot in: The triplet state, ed. A. B. Zahlan (Cambridge Univ. Press, London 1967), p. 125.
[31] W. Hägele, Dissertation Universität Stuttgart (1977).
[32] A. Carrington and A. D. LcLachlan, Introduction to Magnetic Resonance (Harper and Row, New York 1967).
[33] T. J. Schaafsma, J. F. Kleibeuker, R. J. Platenkamp, and P. Geerse, in: Proceedings of the 12th European Congress on Molecular Spectroscopy, eds. M. Grossmann, S. G. Elkomoss, and J. Ringeissen (Elsevier, Amsterdam 1976), p. 491.
[34] J. Kleibeuker, S. J. van der Bent, and T. J. Schaafsma, Paper presented at the 3rd International Seminar on Excitation Energy Transfer in Condensed Matter, Prague 1976.